Dissecting Lysozyme by Single-Molecule Techniques

Issa S. Moody[1], Yongki Choi[2,], Tivoli J. Olsen[1], Patrick C. Sims[2], Mariam Iftikhar[1], William A. Brown[1], Philip G. Collins[2,*], Gregory A. Weiss[1,3,*]
From Departments of Molecular Biology & Biochemistry[1],
Physics and Astronomy[2], and Chemistry[3],
University of California at Irvine, Irvine, California 92697-2025, USA

ABSTRACT

Historically, examination of enzymatic catalysis has largely involved measurements with populations of enzymes *in vitro*. Such studies examine the averaged properties across a large number of molecules. T4 lysozyme, for example, has been extensively studied using conventional, ensemble measurements. The results have uncovered insights into the enzyme's catalytic mechanism, conformational dynamics, and folding. The advent of new single-molecule techniques has significantly extended our knowledge of this enzyme, through examination of previously unobserved lysozyme dynamics.

For example, key aspects of T4 lysozyme from T4 bacteriophage have been elucidated using protein-functionalized nanocircuits. Attaching one lysozyme molecule to a single-walled, carbon nanotube field-effect transistor allows for the detection of minute changes in the circuit conductance, as the enzyme interacts with its peptidoglycan substrate. Random telegraph signals occurring at 15- and 330-Hz distinguish productive substrate binding from nonproductive binding, respectively; such observations confirmed previous results using single-molecule fluorescence techniques. Additionally, electronic measurements performed with different substrates reveal substrate-specific strategies for peptidoglycan processing by lysozyme. Notably, the relative proportion of time lysozyme spends in the productive state dramatically increases from 51 to 88% when

cross-linked (wild-type) substrate is replaced with a chemically synthesized, linear substrate. The observation suggests the substrate's peptide cross-links can trap the enzyme in a nonproductive binding state. Long-duration data sets, which extend well past the capabilities of single-molecule Förster resonance energy transfer (smFRET) measurements, allow for the analysis of normalized variance of open and closed conformation dwell times. This analysis identifies lysozyme as closing with one-step and opening with a multi-step process. In addition, SWNT-FET data identifies lysozyme as a processive enzyme, which cleaves on average 100 glycosidic bonds before returning to a nonproductive binding state. Furthermore, the underlying mechanism of the pH-dependence of lysozyme has been elucidated. Changes to its processive kinetics do not alter lysozyme activity, but rather lysozyme activity varies with respect to pH due to increased time spent in a nonproductive binding state or an inactive conformation.

smFRET measurements performed on T4 lysozyme have identified a previously unreported behavior of enzymes termed bunching. As observed by smFRET, the enzyme bunches protein conformational motions that exhibit similar times-scales during catalysis. Bunching differs from the memory effect observed in proteins; the latter describes the probability of repeated long or short turnover events. Compared to bunching, where durations of conformational motions occupy a narrow time window, the memory effect covers a broader range of time-scales. Bunching results from multiple consecutive Poisson processes associated with the conformational motions stemming from enzyme-substrate complex formation. Lysozyme, for example, proceeds through about six intermediate steps occurring over 19.5 ms. Furthermore, the data supports a model in which the memory effect stems from slow conformational motions.

In addition to enzymatic catalysis, various aspects of protein folding have been examined via single-molecule measurements. The folding pathways of both hen egg white (HEWL) and T4 lysozyme have been studied using different techniques. The propensity for lysozyme to fold via multiple parallel pathways has been documented by such techniques. Interestingly, whereas >85% of HEWL molecules refold through a slow kinetic pathway containing partially folded intermediate states, single-molecule atomic force microscopy (AFM) illustrates that >85% of T4 lysozyme molecules refold in a fast, two-state, all-or-none fashion. Additionally, the T4 lysozyme molecules that refold in a three-state fashion follow a diverse set of pathways. This single-molecule AFM experiment provides evidence for a kinetic partitioning mechanism. The results provide a portrait of the diverse ways proteins fold into their native structure.

In summary, single-molecule studies of lysozyme have uncovered fundamental insights into mechanisms of biocatalysis and protein folding. This chapter reviews such studies involving lysozyme.

INTRODUCTION

Studying enzymes at the single-molecule level offers researchers the advantage of observing reactions from the perspective of the individual removed from the averaging effects of a large population. Such studies shed light on unknown aspects of the monitored process, which are typically hidden due to the difficulty of synchronizing enzyme activities. Furthermore, observation of short-lived intermediates can be achieved through single molecule experiments. For example, smFRET has been used to investigate the conformational dynamics associated with catalysis by adenylate kinase.[1] smFRET has also demonstrated that the protein folding transition path times for fast-folding (e.g., the

WW domain of the formin-binding protein) and slow-folding (e.g., the GB1 domain of protein G) proteins can differ by only a factor of 5.[2] This latter result suggests that when folding actually occurs, it does so at similar rates for fast- and slow-folding proteins. Optical tweezers have been used for single-molecule studies to investigate the affect of peptide bond formation on the Shine-Dalgarno sequence and other processes. The experiments demonstrated that formation of the first peptide bond during translation destabilizes the interaction between the Shine-Dalgarno sequence and the ribosome, likely facilitating ribosome translocation along the mRNA strand.[3]

The Weiss laboratory, in collaboration with the Collins laboratory, has synthesized enzyme nanocircuits with individual proteins attached to single-walled carbon nanotube field effect transistors (SWNT-FETs).[4–6] Such single-molecule electronic circuits allow detection of minute changes in circuit conductance (G). In this way, chemical reactions involving the attached molecule and the surrounding environment can be monitored in real-time. This approach has proven useful for examining lysozyme catalysis by elucidating unexplored and previously invisible aspects of the catalytic mechanism for the attached enzyme.[5]

Lysozyme presents an excellent model system to calibrate a new single-molecule technique. Previous studies of lysozyme have yielded a plethora of mechanistic information and insight into enzyme catalysis.[7–11] As described further below, elegant FRET experiments have two speeds for lysozyme's hinge motion, and described the dynamic and static disorder associated with the enzyme. The latter property, defined as memory, depicts an enzyme with a range of motions from nanoseconds to milliseconds. Lysozyme catalyzes the hydrolysis of the β-1,4 glycosidic bond between N-

acetylmuramic acid (NAM) and N-acetyl-D-glucosamine (NAG), which comprise the peptidoglycan layer found in Gram-positive bacterial cell walls.[12]

Since hydrolysis by lysozyme is well-characterized for ensemble-averaged, large populations of enzymes, bacteriophage T4 lysozyme was used for single-molecule attachment and SWNT-FET studies. Proteins, especially enzymes, are often attached to carbon nanotubes; however, such devices are typically applied to the detection of biomolecules (e.g. glucose, or cancer biomarkers).[13–16] Another approach aims to detect the intermediates, the transition states, and the kinetic parameters inherent to the attached enzyme.

Figure 1. Bacteriophage T4 lysozyme (PDB: 6LZM). The single-cysteine lysozyme variant used for SWNT-FET studies encodes a S90C mutation (red), which serves as the point of conjugation to the SWNT via a maleimide-pyrene linker. Key active site residues are highlighted in blue.

The attachment chemistry used to anchor the enzyme to the SWNT plays a critical role in the sensor properties. Researchers commonly use non-covalent attachment chemistry to adsorb enzymes to SWNT sidewalls. Theoretically, non-covalent attachment should result in the least damage to enzyme structure, as non-covalent binding can leverage existing hydrogen bonds, salt bridges and van der Waals interactions from the surface of the protein. However, without careful selection of a point of attachment not likely to perturb protein conformation, significant decreases in catalytic activity can

occur. For example, after non-covalent, non-specific binding, soybean peroxidase lost 70% of its catalytic activity and α-chymotrypsin lost 99%.[17] Analysis by FT-IR spectroscopy demonstrated that both proteins experienced significant structural changes upon non-specific adsorption to the SWNT sidewalls. Likely partial denaturation of the protein allowed hydrophobic core residues to unfold and interact with the SWNTs.

Using a gene encoding a pseudo wild-type variant of T4 lysozyme lacking cysteine residues (C54T C97A) as a template for mutagenesis, Ser90 was selected for mutagenesis to cysteine (Fig. 1, red residue). With identical numbers of atoms and similar charges at neutral pH, the serine-to-cysteine mutation is conservative, and less likely to alter lysozyme tertiary structure. In addition, the placement of the cysteine residue opposite the active site (Fig. 1, blue residues) should theoretically result in an upward-facing active site, available for substrate binding and release. Using maleimide-pyrene linkers for non-covalent attachment to the SWNT resulted in reliable conjugation during 80% of the fabrication attempts.[5] Using related chemistry, T4 lysozyme has previously been shown to maintain enzymatic activity upon attachment to solid surfaces.[18] Also, smFRET measurements in which lysozyme remained in solution and its peptidoglycan substrate was attached to a surface resulted in similar frequency motions, which demonstrates lysozyme anchored to a surface does not experience significantly altered frequencies of conformational motion.[19]

Device architecture

The SWNT-based FET comprises one single-walled carbon nanotube spanning two electrodes that are entirely passivated with a layer of poly (methyl methacrylate) (PMMA). Electron beam lithography is next used to etch away a 200 nm window,

resulting in a window exposing the SWNT to buffer. The bioconjugation to lysozyme

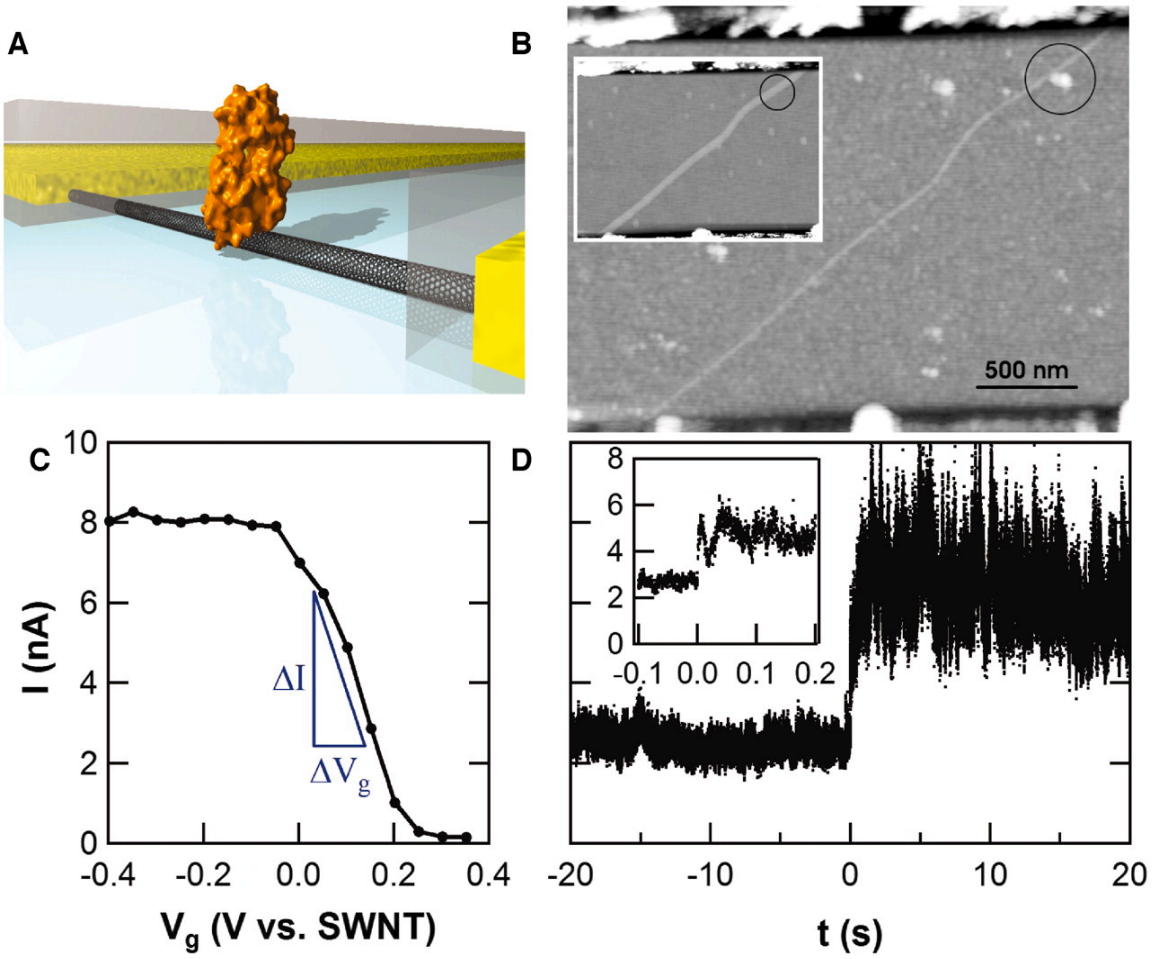

Figure 2. (**A**) Schematic illustration of a single lysozyme molecule incorporated into a nanocircuit. Passivation with PMMA (gray layer), followed by window etching, precedes bioconjugation. (**B**) AFM topography confirms attachment of a single lysozyme molecule. The circle highlights the point of attachment before bioconjugation (inset) and after. (**C**) Measuring the effect of electrolytic gating on a nanotube current (I) allow selection of the precise gate voltage (V_g) for generating high signal-to-noise data. (**D**) Catalytic conformational motions alter nanotube current upon addition of peptidoglycan substrate at t = 0. Magnified time axis in inset. From reference [5]. Reprinted with permission from AAAS.

takes place within this window (depicted in the schematic diagram of Fig. 2A). Atomic force microscopy confirms attachment of a single lysozyme molecule after attachment (Fig. 2B). The one-dimensional nature of SWNTs along with their gate sensitivity at the point of attachment makes the enzyme-functionalized nanodevice highly sensitive to

small changes in the electric field. For example, the movement of charged protein residues close to the SWNT can be transduced into fluctuations in circuit conductance.

Following lysozyme attachment, the effect of electrolytic gating on nanotube current (I) can be measured (Fig. 2C). This plot allows selection of the precise gate voltage (V_g) for generating highest possible signal-to-noise data. As lysozyme hydrolyzes glycosidic bonds, the protein undergoes an 8 Å hinge-bending motion,[11,20,21] ultimately resulting in changes to the nanocircuit current (Fig. 2D). The general concept has been previously described.[22–25]

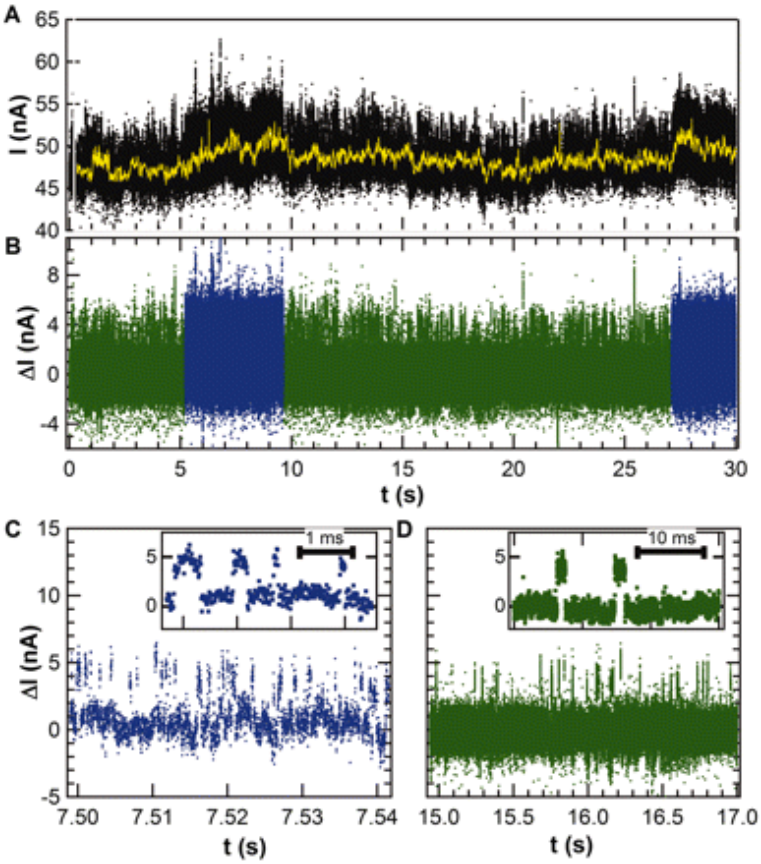

Figure 3. (**A**) Prior to data analysis, 1/*f* noise (yellow) is subtracted from *I*(t) traces to simplify the analysis. (**B**) Dynamic switching, which occurs at two different rates, represents productive (green) and nonproductive (blue) conformational motions, respectively. (**C**) Nonproductive conformational motions occur at 300-Hz, and (**D**) productive conformational motions occur at 15-Hz. The insets illustrate isolated switching events. From reference [5]. Reprinted with permission from AAAS.

Conformational dynamics: pH-dependence

After subtraction of the 1/*f* noise inherent to electronic devices (Fig. 3A), analysis of *I*(t) reveals the presence of a random telegraph signal (RTS) oscillating at two

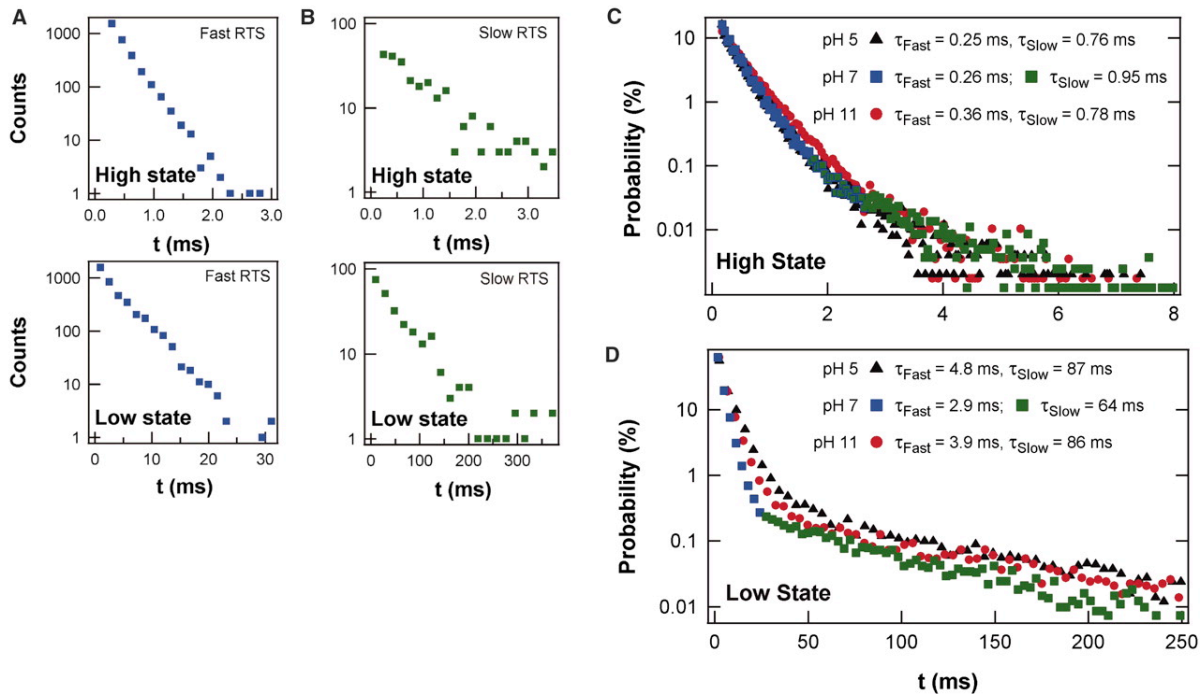

Figure 4. (**A** and **B**) Probability distributions of the high (τ_{hi}) and low (τ_{lo}) state durations during (**A**) fast and (**B**) slow RTS switching show τ_{hi} and τ_{lo} can be fit to a single exponential for periods less than $<t_{mem}>$. (**C** and **D**) Periods greater than $<t_{mem}>$ exhibit biexponential probability distributions as a result of the presence of many fast and slow RTS segments. The color scheme in (**A**) through (**D**) match the Fig. 2 color scheme. Though the high-current state has virtually no pH dependence (**C**), the low-current state is at least 25% faster at pH 7 than at pH 5 or 11 (**D**). From reference [5]. Reprinted with permission from AAAS.

different rates (Fig. 3B). The fast RTS (blue), fluctuating at 316-Hz, oscillates ≈20-fold faster than the slow RTS (green), which fluctuates at 15-Hz. Short-duration I(t) traces further illustrate the fast and slow RTS and clarify the presence of a high current state and low current state. The duration of time spent in the high or low current state, termed τ_{hi} and τ_{lo}, respectively, provide an electronic signature of the lysozyme conformation. For example, analysis of nanocircuit data identifies τ_{hi} as the duration of time lysozyme

spends in a closed conformation; τ_{lo} represents the length of time lysozyme spends in an open conformation. Their sum represents one complete oscillation and defines a mean turnover rate for the activity, $k = (\langle t_{lo} \rangle + \langle t_{hi} \rangle)^{-1}$. The variation in rates observed between different lysozyme molecules reflects static disorder. For example, slow RTS rates varied from 10 – 50 Hz with an average k = 24 ± 15 Hz while fast RTS rates varied from 127 – 461 Hz, with an average k = 284 ± 127 Hz (n = 7). Comparison of these rates with previously published smFRET experiments[19,26] indicates the slow and fast RTS are associated with productive and nonproductive conformational motions, respectively.

Both the fast and slow RTS segments last for several seconds, which suggests the existence of a two-state memory effect. Long-duration data sets enable the accurate determination of the average duration of this memory effect $\langle t_{mem} \rangle$. Analyzing individual fast and slow RTS segments demonstrates that probability distributions for τ_{hi} and τ_{lo} can be fit to a single exponential for periods less than $\langle t_{mem} \rangle$ (Fig. 4A, B). However, periods greater than $\langle t_{mem} \rangle$ exhibit biexponential probability distributions as a result of the presence of many fast and slow RTS segments (Fig. 4C, D).

Analysis of the normalized variance of τ_{hi} and τ_{lo} durations indicate lysozyme opens in at least two steps but closes in a single step.[5] Any single-step Poisson process displays a normalized variance of

$$r = \frac{\sigma^2}{\langle t \rangle^2} = \frac{\sum_i (\tau_i - \langle \tau \rangle)^2}{\sum_i \tau_i^2}$$

and is used to identify hidden intermediate steps in a reaction process.[27–29] The process underlying the transition from I_{lo} (open) to I_{hi} (closed) must be governed by a single step as analysis of t_{lo} durations yield an $r \approx 1$ (Table 1). On the other hand, analysis of t_{hi}

durations yields an $r < 1$, which demonstrates at least two processes govern the transition from I_{hi} to I_{lo}. This is true for transitions occurring during both productive and nonproductive periods.

Table 1. Normalized variances of lysozyme rates.

	Parameter	pH 5	pH 7	pH 11
Processing (slow)	r_{hi}	0.68 ± 0.15	0.74 ± 0.12	0.60 ± 0.15
	r_{lo}	1.00 ± 0.18	1.06 ± 0.15	1.11 ± 0.23
Nonproductive (fast)	r_{hi}	0.48 ± 0.10	0.43 ± 0.06	0.61 ± 0.08
	r_{lo}	0.97 ± 0.13	0.99 ± 0.09	1.00 ± 0.10

From reference [5]. Reprinted with permission from AAAS.

Table 2. Lysozyme activity rates.

	Parameter	pH 5	pH 7	pH 11
Processing	$\langle\tau_{hi}\rangle$, ms	0.76 ± 0.05	0.95 ± 0.08	0.78 ± 0.09
(slow)	$\langle\tau_{lo}\rangle$, ms	87 ± 3.0	64 ± 2.0	86 ± 3.0
	ΔE, kcal/mol	2.84	2.53	2.82
	k, Hz	11.4	15.4	11.5
	$\langle\tau_{mem}\rangle$, s	9.3 ± 5.1	8.0 ± 3.0	12.0 ± 4.4
	% time in state	16.3%	41.1%	21.1%
	time-averaged catalytic rate, Hz	1.8	6.3	2.4
Nonproductive	$\langle\tau_{hi}\rangle$, ms	0.25 ± 0.01	0.26 ± 0.01	0.36 ± 0.01
(fast)	$\langle\tau_{lo}\rangle$, ms	4.80 ± 0.35	2.90 ± 0.10	3.90 ± 0.17
	ΔE, kcal/mol	1.77	1.45	1.43
	k, Hz	198	316	235
	$\langle\tau_{mem}\rangle$, s	6.2 ± 4.0	7.9 ± 2.3	5.4 ± 1.8
	% time in state	72.4%	52.1%	63.8%
Inactive	$\langle\tau_{mem}\rangle$, s	0.83 ± 0.63	0.72 ± 0.25	0.96 ± 0.53
	% time in state	11.3%	6.8%	15.0%
	Processing Ineffective Inactive	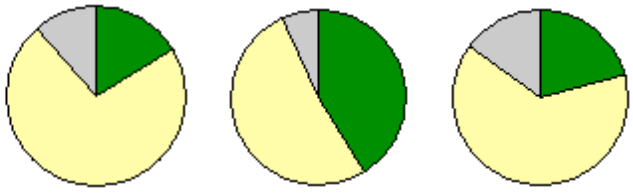		

From reference [5]. Reprinted with permission from AAAS.

Boltzmann statistics provide the thermodynamic probability of the enzyme being in either the open or closed conformation as $\Delta E = k_B T \ln(\langle\tau_{hi}\rangle / \langle\tau_{lo}\rangle)$. τ_{lo} is 20-fold slower in productive periods than in nonproductive periods and ΔE is 1.1 kcal/mol greater in productive periods than in nonproductive periods. This is consistent with τ_{lo} representing the open conformation, as successful bond protonation requires sufficient time and energy.

Nanocircuit data elucidates the degree to which pH alters lysozyme activity. At neutral pH, lysozyme spends, on average, 64 ms in its open configuration and about 1 ms in its closed conformation as it hydrolyzes substrate bonds. The rate of the enzymes processive kinetics decreases from 15.4 Hz at pH 7 to ≈11.4 Hz at pH 5 and 11 (Fig. 4C, D). However, this decrease in *k* is relatively insignificant and only minimally contributes to changes in the enzyme's activity. Nanocircuit data identifies increased time spent in the nonproductive binding state as the dominant contributing factor to decreased enzymatic activity (Table 2). At pH 7, the optimal pH for activity, lysozyme spends 41% of its time in a productive conformation, 52% of its time in its nonproductive conformation, and 7% of its time in an inactive state. Away from pH 7, the time lysozyme spends in its productive conformation is drastically reduced to 16% and 21% at pH values 5 and 11, respectively. In addition, the time spent in the inactive conformation doubles.[5]

Conformational dynamics: Substrate interactions

Proteins access many conformations associated with energy minima along their free energy landscape. These equilibrium conformational motions occur spontaneously as a function of kT and the frequency at which they populate different conformations depends on the energy barrier between conformations.[30] In contrast, substrate binding drives non-equilibrium protein conformational motions. MD simulations indicate the driving force for enzyme-substrate complex formation is electrostatic interactions between positively charged lysozyme residues and negatively charged moieties of the peptidoglycan substrate.[31] Substrate binding potentially shifts the equilibrium towards specific conformations resulting in increased time spent in one state over another.

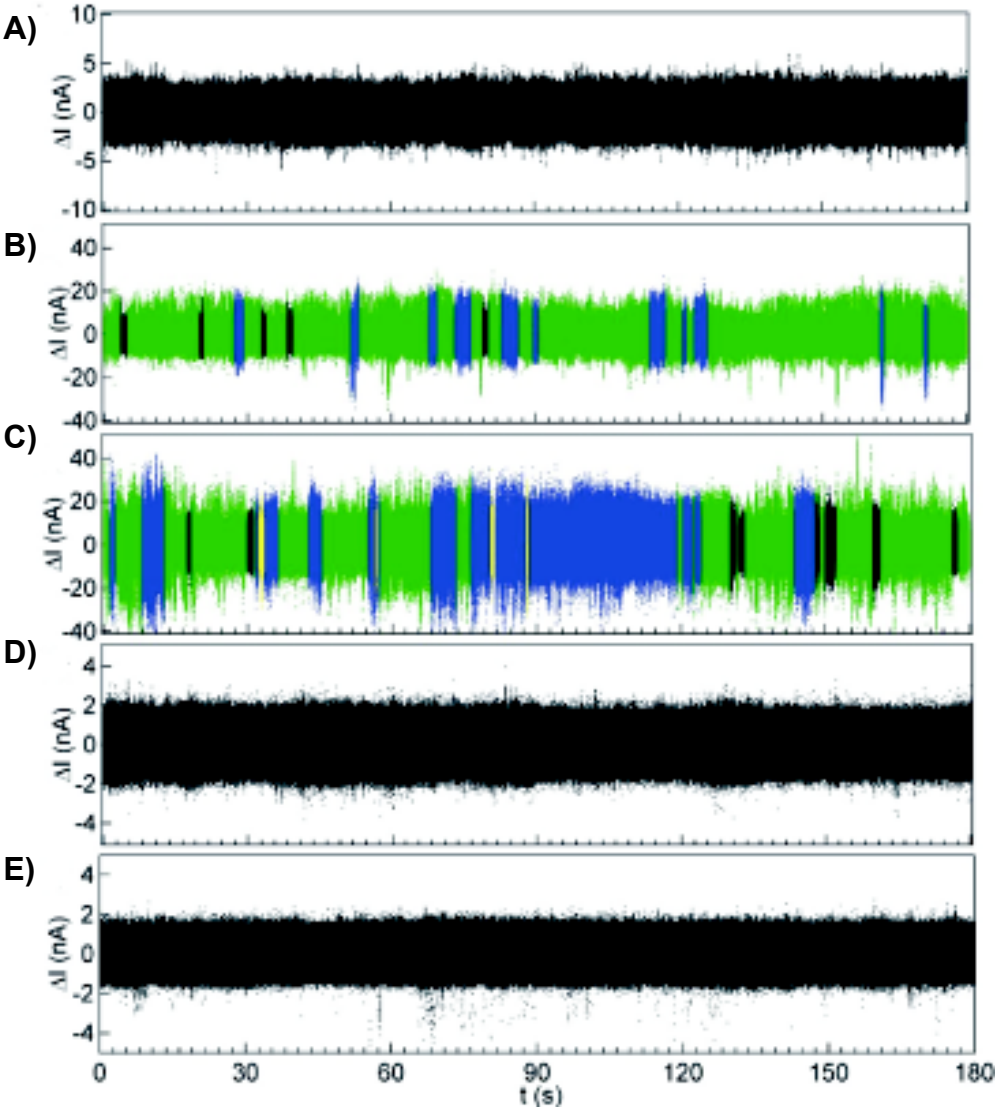

Figure 6. (**A**) No switching arises when measurements are recorded in phosphate buffer lacking substrate. The percentage of time lysozyme spends in a productive state or nonproductive state differs between (**B**) linear substrate and (**C**) cross-linked peptidoglycan. Cross-linked substrate elicits no *I(*t) response from an inactive (**D**) E11H variant and an inactive (**E**) T26E variant. Reprinted with permission from reference [6]. Copyright (2012) American Chemical Society.

In the case of lysozyme, nanocircuit measurements demonstrate that the peptidoglycan substrate can play a crucial role in shifting the equilibrium between different lysozyme conformational states. Using a chemically synthesized, linear version

of peptidoglycan (Fig. 5) allows lysozyme to spend significantly more time in its productive binding state when compared to wild-type substrate (Fig. 6B, C). Wild-type peptidoglycan includes pentapeptide crosslinks. Such structures do not hinder lysozyme processivity, but do alter its time spent hydrolyzing substrate bonds.

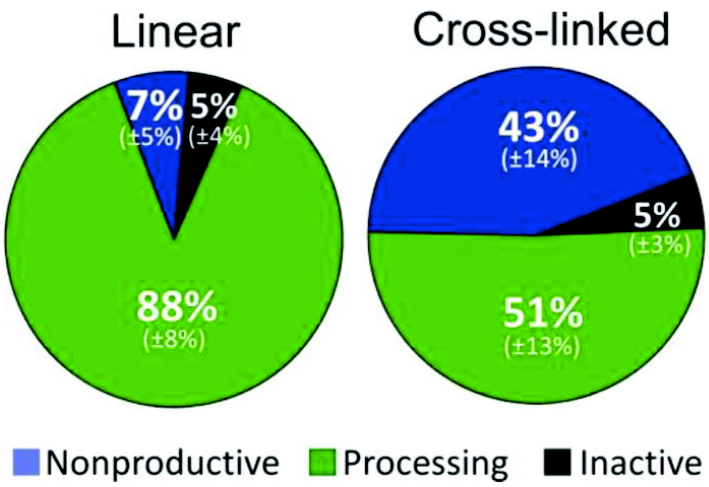

Figure 7. Proportion of time lysozyme spends in different states to process linear or cross-linked substrate. Standard deviations are indicated in parentheses (n = 6 for the linear substrate and n = 8 for the cross-linked substrate). Reprinted with permission from reference [6]. Copyright (2012) American Chemical Society.

Lysozyme spends 51% of its time in a productive state when digesting cross-linked peptidoglycan and 88% of its time in a productive state when digesting linear substrate (Fig. 7). The enzyme spends 7% of the time trapped in its nonproductive binding state when digesting linear substrate, and significantly increases its time to 43%, when the enzyme digests cross-linked substrate. Lysozyme spends similar amounts of time in an inactive conformation (≈1 s) for both linear and cross-linked substrate. Linear substrate results in slightly increased kinetic rates as well. Cross-linked peptidoglycan is processed at 30 Hz whereas linear peptidoglycan is processed at 36 ± 18 Hz, though the error in the measurement could invalidate this conclusion. Nonproductive motions oscillate at 287 and 329 Hz for cross-linked and linear peptidoglycan, respectively. The additional slowing of the nonproductive motions is consistent with a model in which the enzyme

transits from one polysaccharide to another parallel polysaccharide at cross-linked points.[32]

Because productive periods are always interrupted by inactive periods and nonproductive periods are never interrupted by inactive periods, nanocircuit data suggests lysozyme hydrolyzes substrate bonds processively until it reaches the end of a polymeric chain (Fig. 6B, C). Additionally, inactive periods are always followed by productive periods regardless of substrate type; the observation supports a model in which lysozyme hydrolyzes many consecutive bonds before dissociating from the substrate. Nanocircuit data also identifies a behavior in which lysozyme remains substrate-bound in a closed (high $G(t)$), inactive conformation. This type of behavior, which occurs only during nonproductive binding and with cross-linked substrate, tends to last 0.5 – 3 s (Fig. 6C, yellow).[32] The presence of the fast and slow RTS is dependent on the presence of an attached, catalytically active lysozyme and peptidoglycan substrate, as the phosphate buffer alone yields no changes in nanocircuit conductance (Fig. 6A). Control measurements in which catalytically inactive lysozyme variants were incorporated into nanocircuits and subjected to peptidoglycan substrate did not exhibit fluctuations in conductance (Fig. 6D, E).

Conformational dynamics: smFRET

The conformational dynamics and catalytic mechanism of lysozyme have been explored using smFRET and ensemble FRET measurements. For example, labeling two cysteine residues with Texas Red and tetramethylrhodamine (Fig. 8A) allowed Lu and coworkers to measure fluctuations in fluorescence derived from conformational motions induced by substrate binding. Fig. 8B illustrates the decrease in fluorescence associated

with substrate binding. Lysozyme molecules in this bulk control assay, on average, spend more time in a closed, substrate-bound conformation, resulting in increased inter-fluorophore distance and decreased FRET efficiency.[33]

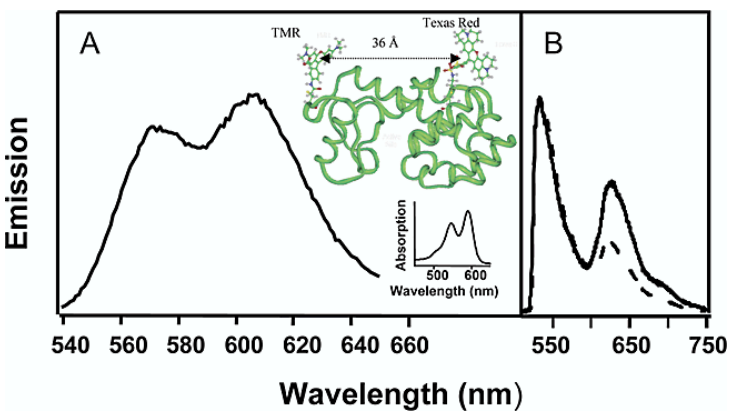

Figure 8. Ensemble-averaged spectroscopy control results. (**A**) Fluorescence spectra of tetramethylrhodamine- and Texas Red-labeled 240 nM T4 lysozyme excited at 530 nm. The absorption spectrum is plotted in the inset. The crystal structure of wild-type T4 lysozyme with two dye molecules is shown in a second inset. (**B**) Fluorescence spectra of Alexa 488/Alexa 594-labeled T4 lysozyme mutant (E11A) excited at 488 nm. The solid and dashed lines are the fluorescence spectra of the enzyme in solution without and with substrate *E. coli* B cell walls present, respectively. The two spectra are normalized to the same maximum point to aid the view. Reprinted with permission from reference [31]. Copyright (2003) American Chemical Society.

Extending this strategy to the single-molecule landscape involved attaching labeled lysozyme molecules to a modified glass surface and using an inverted fluorescence microscope. Fluorescence trajectories from smFRET experiments illustrate lysozyme hinge bending in the presence of peptidoglycan (Fig. 9). Lu and coworkers attribute each oscillation in the fluorescence intensity to the hinge-bending motion associated with substrate bond hydrolysis or a nonproductive binding and release event. Using 50% of the bimodal intensity distribution as a threshold value, the durations of activated complex formation times were measured. The formation times populate a Gaussian distribution with a mean time of 19.5 ms and a standard deviation of 8.3 ± 2 ms (Fig. 10). The Gaussian distribution and small, incremental spikes in fluorescence intensity implies lysozyme transitions through several intermediate states as the enzyme forms the

activated complex, an expectation also supported by computational modeling.[31] Single-molecule nanocircuit data confirmed these measurements, as analysis of the normalized variance of τ_{hi} and τ_{lo} durations indicate lysozyme opens in at least two steps but closes in

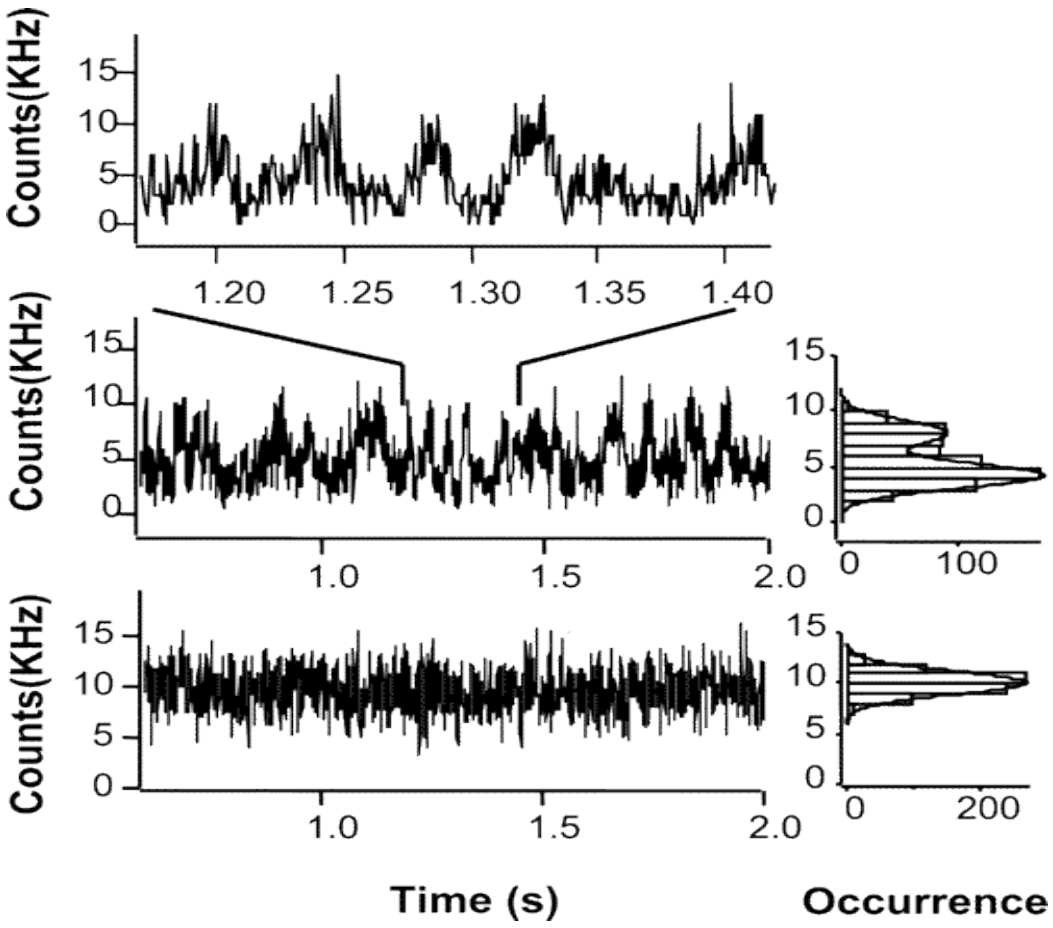

Figure 9. Simultaneous probing of a single T4 lysozyme enzymatic reaction turnover trajectory with correlated hinge-bending conformational motions of the enzyme under hydrolysis of the polysaccharide of a cell wall. The data in the three panels were recorded in 0.65 ms per channel at the same enzymatic reaction condition. The upper panel shows an expanded portion of a trajectory (middle panel) from donor fluorescence of a donor-acceptor-labeled single T4 lysozyme. Intensity wiggles in the trajectory are evident beyond the measurement shot noise. The lower panel shows a portion of a trajectory recorded from a donor- only-labeled enzyme. The fluorescence intensity distributions derived from the two trajectories are shown in the insets of the middle and lower panels. The solid lines are fit using bimodal and Gaussian functions, respectively. Reprinted with permission from reference [31]. Copyright (2003) American Chemical Society.

a

single step.[5] Taken together, these data may suggest the time required for substrate

dissociation dominates the catalytic lifecycle despite the fact that smFRET experiments suggest no major structural rearrangements occur during substrate dissociation.[31]

smFRET measurements performed on T4 lysozyme have identified a previously unreported enzyme behavior termed *bunching*, which is characterized by the clustering of conformational motion durations during catalysis. Bunching differs from the memory effect observed in proteins, which describes the probability of repeated long or short turnover events. Compared to bunching, where durations of

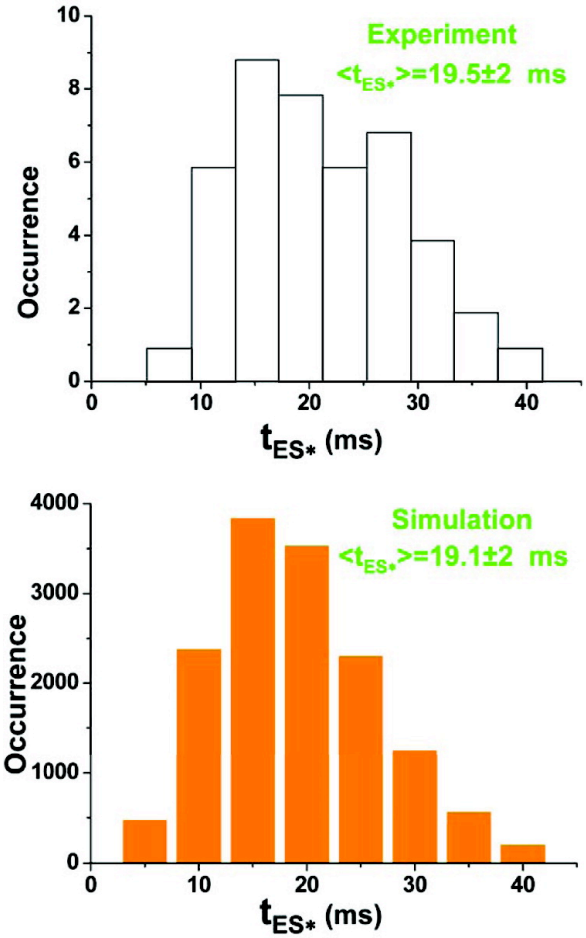

Figure 10. Histograms of the experimental[31] and simulated formation times (t_{ES*}) of the conformational motions in forming ES*. The experimental data is deduced from a single T4 lysozyme fluorescence trajectory.[31] t_{ES*} is the duration time of each wiggling of the intensity trajectory above a threshold. The threshold is determined by 50% of the bimodal intensity distribution.[31] The mean formation times, $<t_{ES*}>$, are 19.5 ± 2 and 19.1 ± 2 ms for the experiment and simulation, and the corresponding standard deviation of the formation time is 8.3 ± 2 and 7.5 ± 2 ms, respectively. Reprinted with permission from [31]. Copyright (2003) American Chemical Society.

conformational motions occupy a narrow time window, the memory effect covers a broader range of enzyme time-scales. Bunching results from multiple consecutive Poisson processes associated with conformational motions stemming from enzyme-substrate complex formation. Bunching likely evolved as a mechanism for increasing the catalytic efficiency of enzymes.[26,33]

Extensive study has been performed on dihydrofolate reductase (DHFR), which reduces dihydrofolate to tetrahydrofolate, and the enzyme offers an excellent system to examine the interplay between equilibrium conformational motions and catalysis. A combination of experimental and computational measurements illustrates the presence of coupled networks of thermally regulated conformational motions. Coupled motions forming a series of enzyme-substrate configurations to facilitate substrate turnover could potentially be a general characteristic of enzymes.[34] However, this interpretation is disputed, as some research suggests electrostatic preorganization is the dominant contributing factor to catalysis, not conformational motions.[35] In any event, computational modeling suggest such networks may play an integral part in lysozyme catalysis.[31,33] Conformational motion times clustering together during activated complex formation could increase the catalytic efficiency of lysozyme by ensuring specific conformations are adjacent to one another along the reaction pathway.

Protein folding

Single-molecule atomic force microscopy reveals previously unidentified characteristics of folding pathway followed by lysozyme.[36] Li and coworkers interrogated the unfolding and refolding pathway of T4 lysozyme using an AFM-applied mechanical force. For this experiment, Li and coworkers constructed a polyprotein comprised of a

cysteine-free lysozyme variant flanked by 4 GB1 protein domains on both sides. GB1 is well characterized, and has been previously reported to unfold with 180 pN of force. Using GB1 domains as a signature for lysozyme unfolding, Li and coworkers were sure lysozyme was unfolded if at least five force extension peaks, with four corresponding to GB1 domains, were present in the force extension diagram. The repetitive unfolding-refolding of lysozyme illustrates that 87% of lysozyme molecules unfold in an all-or-none fashion, and 13% unfold in a three-state fashion. Although evidence is limited for a kinetic partitioning mechanism to explain protein folding, this work directly supports the kinetic partitioning model.

Many local energy minima exist along a protein's unfolding pathway.[30] The vast majority of lysozyme molecules undergo two-state unfolding. However, the same molecule can exhibit both two- and three-state unfolding, suggesting the tendency to proceed through multiple folding pathways is an intrinsic property of lysozyme. Contour-length increments ΔLC from force extension curves indicate lysozyme completely unfolds to ΔL_C = 59 nm with an average force of 50 pN. Computational modeling to better characterize lysozyme's unfolding pathway indicates the unfolding distance $\Delta\chi$ between the folded state and transition state is 0.75 nm. Helix A (residues 1-11) associates with the C-terminal lobe of lysozyme and $\Delta\chi$ = 0.75 nm is consistent with the unfolding of N-terminal helix A from the C-terminal lobe. Although precise assignment of the location of the energy barrier cannot be determined due to AFM resolution limitations, the disruption of the interaction between N-terminal helix A and the C-terminal lobe is likely the dominant kinetic barrier between the N- and C-terminal lobes.

Lysozyme molecules that unfold in a three-state fashion (≈13%) can do so through various pathways, as evidenced by distinct force extension curves (Fig. 13). For example, one molecule exhibits ΔL_{C1} = 16 nm and ΔL_{C2} = 43 nm, and another molecule unfolds with ΔL_{C1} = 51 nm and ΔL_{C2} = 13 nm. The first unfolding event, corresponding to ΔL_{C1}, results in the molecule transiently populating a kinetically stable intermediate state before the second unfolding event occurs. Three-state unfolding indicates several distinct kinetic barriers exist along the lysozymes unfolding pathway; however, three specific pathways dominate. ΔL_{C2} values equal to 14, 29, and 46 nm support a model in which the second kinetic energy barrier is 45, 30, and 13 nm away from its resting length between the N- and C-termini. Despite differences in ΔL_{C1} and ΔL_{C2}, the forces required for each unfolding event remain very similar, clustering around 50 pN.

To further characterize the impact of the helix A-C-terminal lobe interaction, Li and coworkers performed similar unfolding experiments with PERM1, a circularly permutated lysozyme mutant in which helix A has been removed from the N-terminus and fused to the C-terminus of the protein. Despite maintaining a nearly identical structure to wild-type lysozyme, PERM1 exhibited very different unfolding properties (Fig. 14). For example, approximately one fifth of T4 lysozyme molecules (n=190) did not display unfolding peaks, meaning the unfolding event occurred outside of the resolution of the AFM instrument (i.e., at force values <20 pN). The majority of lysozyme molecules (≈56%) unfolded in a single step with ΔL_C values ranging from 20 – 60 nm. As compared to wild-type lysozyme (≈13%), an increased proportion of molecules unfolded in a three-state fashion (≈24%). Unfolding characteristics of the circular permutant underscore the importance of the interactions between N-terminal

residues and helix A. This broad distribution supports a model in which lysozyme molecules do not unfold from one particular intermediate conformation but rather the lysozyme molecules briefly occupy one of many possible intermediate conformations.

Taken together, these data elucidate aspects of lysozyme folding not previously reported and provide strong evidence in support of a kinetic partitioning mechanism as a model for explaining how proteins fold into their three dimensional structures. However, multiple possible models exist to account for the observation of a kinetic partitioning mechanism for lysozyme. Additional experiments may be required to confirm the underlying cause of the kinetic partitioning mechanism. For example, in one situation, lysozyme exists as folding intermediates of structurally homogeneous species. In this case, mechanical manipulation of lysozyme most frequently results in two-state unfolding. In the case of three-state unfolding, lysozyme proceeds through various local energy minima, getting trapped along the way to the unfolded state. Lysozyme existing as a heterogeneous species reflects the second possible scenario. In this scenario, lysozyme molecules, comprising both two- and three-state unfolding populations, result from disparate three-dimensional conformations already existing prior to mechanical force stimulation. Of course, for this scenario to occur, the experiments showing the same lysozyme molecule unfolding in both two and three steps must mean the molecule refolds into a different native conformation with each unfolding event. Without direct evidence supporting this second hypothesis, Li and coworkers propose the first possibility as the most likely scenario.

Ensemble-level folding experiments performed with native state hydrogen exchange depict lysozyme as having a range of stabilities. The distribution of unfolding

free energies of lysozyme forms a continuum of stabilities across the molecule. Because the hierarchical organization of conformations does not support the conventional theories of the folding pathway of lysozyme, the experiment challenges our understanding of protein folding and energy landscapes. The continuum of stabilities across lysozyme is consistent with single-molecule AFM experiments, which illustrate a broad distribution of unfolding trajectories. The broad distribution of unfolding trajectories further supports a model in which lysozyme does not unfold from a defined intermediate state, but from one of many potential intermediate states.[37]

In addition to protein unfolding and folding, AFM has been used to directly measure enzymatic activity of HEW lysozyme molecules adsorbed on a mica surface. Height fluctuations of approximately 1 nm were observed after addition of substrate and disappeared after addition of an inhibitor. The ≈50 ms duration height perturbations likely resulted from catalysis-associated conformational motions.[38]

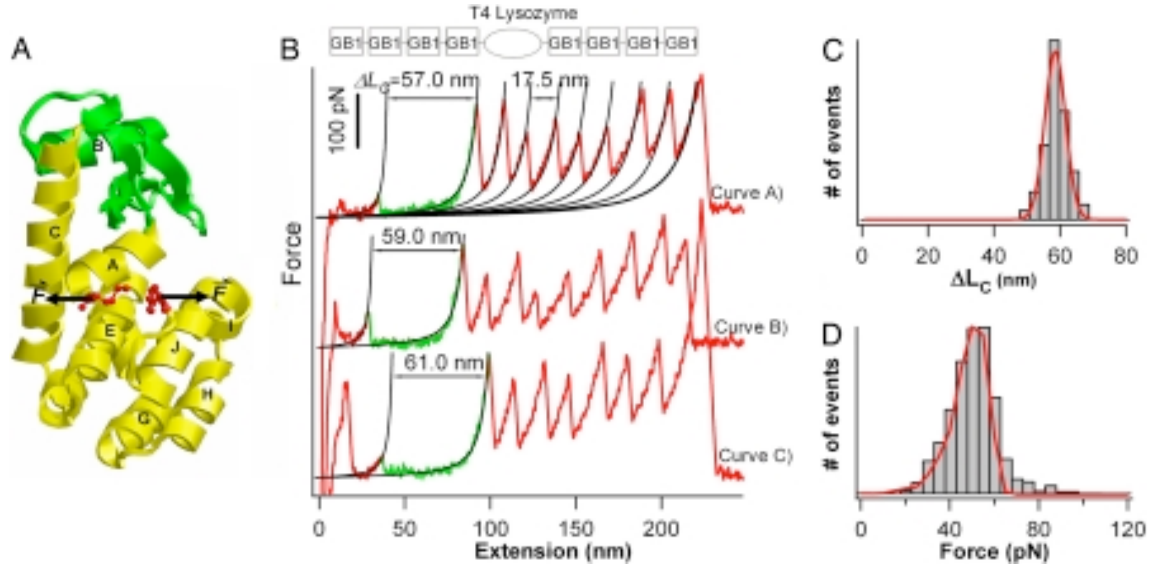

Figure 11. Majority of T4 lysozyme molecules unfold in an apparent all-or-none fashion. (**A**) Tertiary structure of T4L* (PDB ID code 1L63). The N-terminal lobe is green, and the C-terminal lobe and the helix A are yellow. Residues 1 and 164, from which T4 lysozyme is being pulled to unfold, are shown as ball and sticks. Arrows indicate the force acting on T4L*. (**B** Upper) Schematic illustration of the polyprotein chimera $(GB1)_4$-T4L*-$(GB1)_4$ used in single-molecule AFM experiments. (**B** Lower) Typical force-extension curves of polyprotein $(GB1)_4$-T4L*-$(GB1)_4$. The mechanical unfolding events of the well-characterized GB1 domains (red) occurred at ≈180 pN with ΔL_C of ≈18 nm and serve as fingerprints to discern signatures of the mechanical unfolding of T4L*. The unfolding of T4L* always precedes the unfolding of GB1 domains and is characterized by unfolding forces of ≈50 pN and ΔL_C of ≈60 nm, which corresponds to the complete unfolding of T4L* (green). The mechanical unfolding of the majority of T4L* molecules occurs in an apparent two-state fashion. Black lines correspond to WLC fits to the experimental data. (**C**) Histogram of ΔL_C for T4L* molecules that unfold in two-state fashion. Red line is the Gaussian fit to the experimental data with average ΔL_C of 59.0 ± 4.0 nm (n = 1,269). (**D**) Unfolding force histogram for T4L* molecules that unfold in two-state fashion (pulling speed: 400 nm/s, n = 1,269). Red line is the Monte Carlo fit, using an α_0 of 0.055 s^{-1} and a Δx_u of 0.75 nm. Reprinted with permission from [36]. Copyright (2008) National Academy of Sciences, U.S.A.

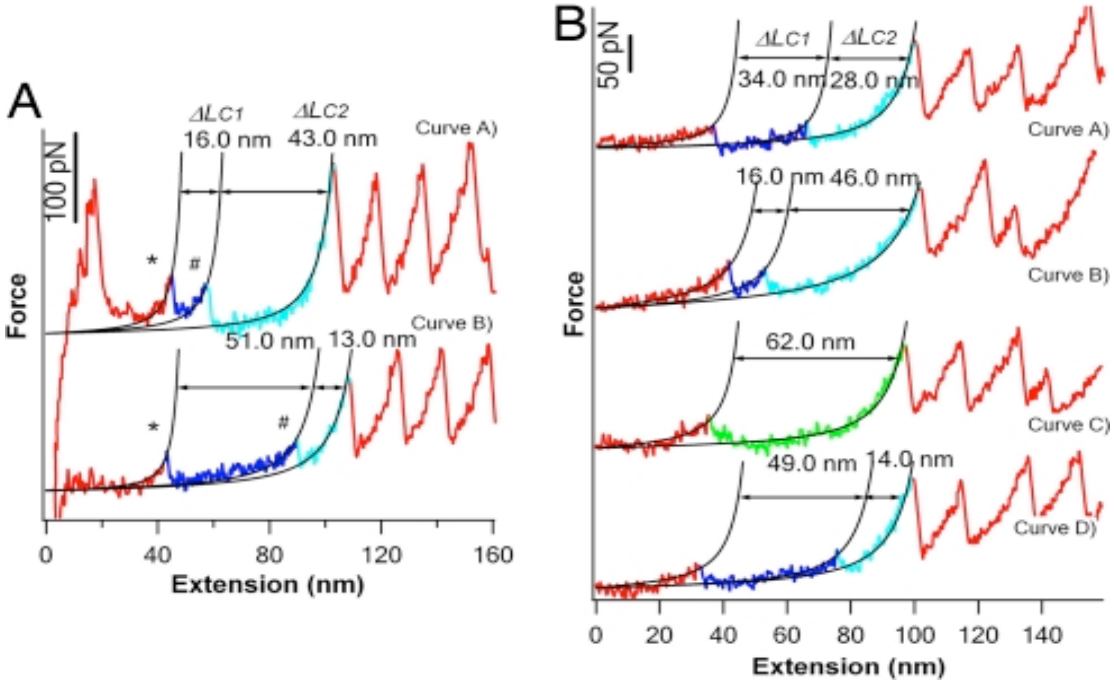

Figure 12. T4 lysozyme can unfold by multiple parallel three-state unfolding pathways. (**A**) Typical force-extension curves of T4L* showing three-state unfolding behaviors. The initial partial unfolding events, which correspond to the unfolding event from the native state to the unfolding intermediate state, are shown in blue, and the subsequent unfolding events, which correspond to the unfolding of the intermediate state to the fully unfolded state, are cyan. WLC fits (black lines) to the experimental data reveal distinct patterns of ΔL_{C1} and ΔL_{C2}. (**B**) A series of force-extension curves of the same T4L* measured during repeated stretching–relaxation experiments. The same T4L* molecule exhibited distinct mechanical unfolding pathways, including the two-state pathway and multiple distinct three-state unfolding pathways. For all of the events showing three-state unfolding behaviors, the sum of ΔL_{C1} and ΔL_{C2} is close to ≈60 nm, which is in agreement with that expected from the complete unfolding of T4L*. Reprinted with permission from [36]. Copyright (2008) National Academy of Sciences, U.S.A.

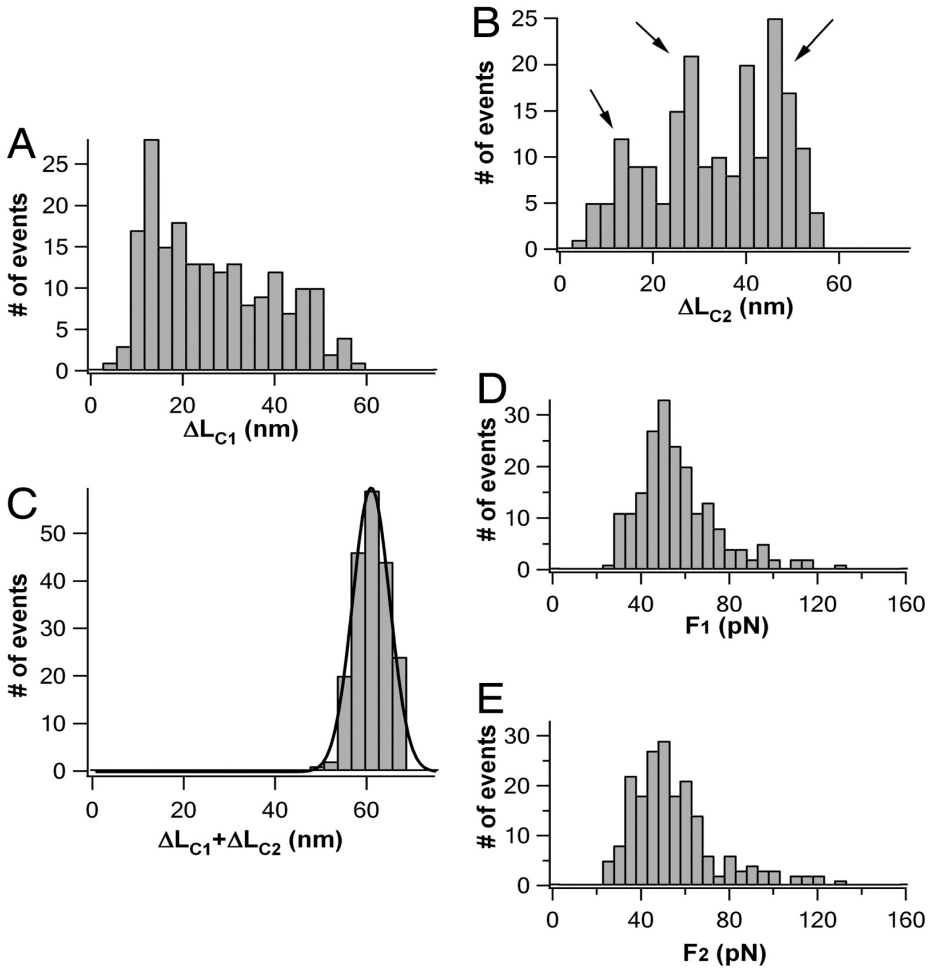

Figure 13. Histogram of ΔL_{C1} (**A**) and ΔL_{C2} (**B**) in three-state unfolding trajectories. For comparison, the histogram of $\Delta L_{C1} + \Delta L_{C2}$, which was measured from the same unfolding trajectories of T4L*, is shown in C. It is evident that ΔL_{C1} and ΔL_{C2} show broad distribution, indicating broad distribution of unfolding pathways for T4L*. Solid line in C is the Gaussian fit to the experimental data with an average $\Delta L_{C1} + \Delta L_{C2}$ of 61.0 ± 4.0 nm (n = 196). (**D** and **E**) Unfolding-force histograms of the first (**D**) and second (**E**) unfolding events of T4L* observed in three-state unfolding pathways. Reprinted with permission from [36]. Copyright (2008) National Academy of Sciences, U.S.A.

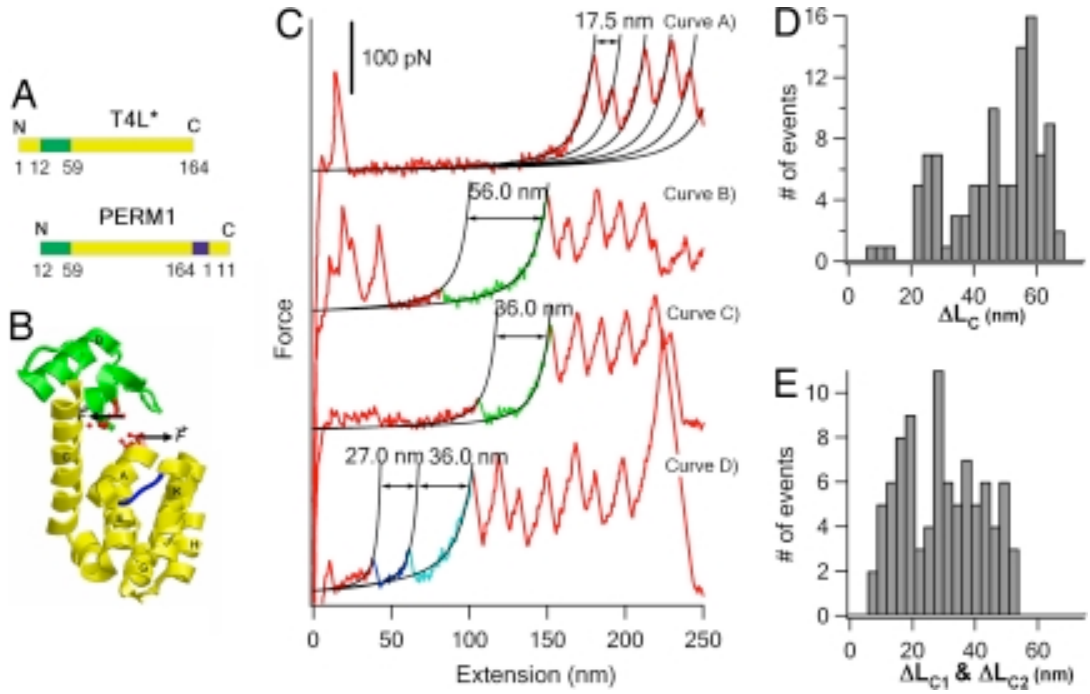

Figure 14. Mechanical unfolding behaviors of circular permutant PERM1. (**A** and **B**) The sequence (**A**) and three-dimensional structure (**B**) of PERM1 are shown. In the circular permutant PERM1, the sequence of helix A is relocated to the C terminus of the whole sequence, and the two subdomains are decoupled. For clarity, the N-terminal lobe is in green and the C-terminal lobe is in yellow. The new N and C termini, from which PERMI is pulled to unfold, are shown in red and ball-and-stick representation. (**C**) Representative force-extension curves of polyprotein chimera $(GB1)_4$-PERM1-$(GB1)_4$. The mechanical unfolding of PERM1 shows diverse unfolding behaviors. PERM1 in curve A did not show clear unfolding force peaks, indicating that it unfolded at low forces below our detection limit. PERM1 in curves B and C corresponds to the two-state unfolding of a fully folded or partially folded PERM1. Curve D shows a three-state unfolding event of PERM1. (**D**) Histogram of ΔL_C for the PERM1 molecules that unfold in two-state fashion (n = 107). (**E**) Histogram of ΔL_{C1} and ΔL_{C2} for PERM1 molecules that unfold in three-state fashion (n = 45). Reprinted with permission from [36]. Copyright (2008) National Academy of Sciences, U.S.A.

CONCLUSION

The advent of single-molecule techniques (e.g., enzyme-functionalized nanocircuits, FRET, optical tweezers, and AFM) allows the elucidation of a wide-range of parameters governing protein function.[2,3,36,39,40] Many studies have focused on investigating enzymatic catalysis, and folding into the protein's three-dimensional structures.[5,26,31,32,36] Lysozyme has provided a key enzyme for such studies.

The conformational dynamics of T4 lysozyme, for example, has been rigorously investigated using smFRET. The studies have distinguished static disorder from dynamic disorder. smFRET experiments with lysozyme allow the observation of catalytic activities associated with individual lysozyme conformers; the activities amongst T4 lysozyme molecules accessing different conformers can vary by 5-fold. Ultimately, smFRET studies of lysozyme identified a new enzyme behavior termed bunching. The inherently asynchronous nature of individual turnover events in ensemble measurements masks such behavior, thus highlighting the importance of single-molecule studies.

In conjunction with smFRET measurements, molecular dynamics simulations suggest lysozyme proceeds through approximately six intermediate steps, as the enzyme forms an activated complex with its peptidoglycan substrate.[19,26,31,33] Data generated from nanocircuit measurements is also consistent with this hypothesis. Though FRET is a very powerful technique, the intrinsic properties of fluorescence limit its use for certain applications. For example, photobleaching restricts the amount of time an individual fluorophore-labeled molecule can be monitored before loss of the signal.

A newly developed technique used lysozyme as a model system, and featured individual copies of the protein attached to a SWNT-FET. By correlating fluctuations in

SWNT-FET conductance with protein conformational motion, a single enzyme could be monitored for extended periods of time (>30 min). The following three observations with this system demonstrates the power of the approach to uncover key insights into enzyme function. First, lysozyme was found to be a processive enzyme. Second, lysozyme exhibits single-step hinge closure and multi-step opening. Third, the basis for the enzyme's pH-dependence was shown to be due to increased time spent in a nonproductive binding state or an inactive state at non-optimal pH values.

The SWNT-FET method offers investigators a new approach for monitoring interactions between binding partners (e.g., enzyme-substrate, enzyme-inhibitor, protein-protein, and others). Future nanocircuit experiments performed with enzyme variants associated with disease states could offer new insight into the catalytic mechanism of the attached protein. In addition, nanocircuit experiments performed with enzyme inhibitors could illuminate mechanisms of inhibition by different antagonists. Ultimately, the use of nanocircuit devices for improving enzymes and their agonists and antagonists offers a new and exciting frontier for biochemical research.

REFERENCES

1. Hanson, J.A. *et al.* Illuminating the mechanistic roles of enzyme conformational dynamics. *Proceedings of the National Academy of Sciences of the United States of America* **104**, 18055-18060 (2007).

2. Chung, H.S., McHale, K., Louis, J.M. & Eaton, W.A. Single-Molecule Fluorescence Experiments Determine Protein Folding Transition Path Times. *Science* **335**, 981-984 (2012).

3. Uemura, S. *et al.* Peptide bond formation destabilizes Shine-Dalgarno interaction on the ribosome. *Nature* **446**, 454-457 (2007).

4. Goldsmith, B.R. *et al.* Conductance-controlled point functionalization of single-walled carbon nanotubes. *Science* **315**, 77-81 (2007).

5. Choi, Y. *et al.* Single-Molecule Lysozyme Dynamics Monitored by an Electronic Circuit. *Science* **335**, 319-324 (2012).

6. Choi, Y. *et al.* Single-molecule dynamics of lysozyme processing distinguishes linear and cross-linked peptidoglycan substrates. *Journal of the American Chemical Society* **134**, 2032-5 (2012).

7. Blake, C.C. *et al.* Structure of hen egg-white lysozyme. A three-dimensional Fourier synthesis at 2 Angstrom resolution. *Nature* **206**, 757-761 (1965).

8. Delepierre, M. *et al.* Electrostatic effects and hydrogen exchange behaviour in proteins. The pH dependence of exchange rates in lysozyme. *Journal of Molecular Biology* **197**, 111-130 (1987).

9. Post, C.B. *et al.* Molecular dynamics simulations of native and substrate-bound lysozyme. A study of the average structures and atomic fluctuations. *Journal of Molecular Biology* **190**, 455-479 (1986).

10. Jacobson, R.H., Matsumura, M., Faber, H.R. & Matthews, B.W. Structure of a stabilizing disulfide bridge mutant that closes the active-site cleft of T4 lysozyme. *Protein Science* **1**, 46-57 (1992).

11. Faber, H.R. & Matthews, B.W. A mutant T4 lysozyme displays five different crystal conformations. *Nature* **348**, 263-266 (1990).

12. Meroueh, S.O. *et al.* Three-dimensional structure of the bacterial cell wall peptidoglycan. *Proceedings of the National Academy of Sciences of the United States of America* **103**, 4404-4409 (2006).

13. Briman, M. *et al.* Direct electronic detection of prostate-specific antigen in serum. *Small Weinheim an der Bergstrasse Germany* **3**, 758-762 (2007).

14. Chen, R.J., Zhang, Y., Wang, D. & Dai, H. Noncovalent sidewall functionalization of single-walled carbon nanotubes for protein immobilization. *Journal of the American Chemical Society* **123**, 3838-3839 (2001).

15. Dai, Z. *et al.* Nanoparticle-based sensing of glycan-lectin interactions. *Journal of the American Chemical Society* **128**, 10018-10019 (2006).

16. Lin, J., Qu, W. & Zhang, S. Disposable biosensor based on enzyme immobilized on Au-chitosan-modified indium tin oxide electrode with flow injection amperometric analysis. *Analytical Biochemistry* **360**, 288-293 (2007).

17. Karajanagi, S.S., Vertegel, A.A., Kane, R.S. & Dordick, J.S. Structure and Function of Enzymes Adsorbed onto Single-Walled Carbon Nanotubes. *Langmuir* **20**, 11594-11599 (2004).

18. Heredia, K.L. *et al.* In situ preparation of protein-"smart" polymer conjugates with retention of bioactivity. *Journal of the American Chemical Society* **127**, 16955-16960 (2005).

19. Hu, D. & Lu, H.P. Placing single-molecule T4 lysozyme enzymes on a bacterial cell surface: toward probing single-molecule enzymatic reaction in living cells. *Biophysical Journal* **87**, 656-661 (2004).

20. Arnold, G.E., Manchester, J.I., Townsend, B.D. & Ornstein, R.L. Investigation of domain motions in bacteriophage T4 lysozyme. *Journal of biomolecular structure dynamics* **12**, 457-474 (1994).

21. De Groot, B.L., Hayward, S., Van Aalten, D.M., Amadei, A. & Berendsen, H.J. Domain motions in bacteriophage T4 lysozyme: a comparison between molecular dynamics and crystallographic data. *Proteins* **31**, 116-127 (1998).

22. Star, A., Gabriel, J.-C.P., Bradley, K. & Grüner, G. Electronic Detection of Specific Protein Binding Using Nanotube FET Devices. *Nano Letters* **3**, 459-463 (2003).

23. Star, A. *et al.* Electronic detection of the enzymatic degradation of starch. *Organic Letters* **6**, 2089-2092 (2004).

24. Besteman, K., Lee, J.-O., Wiertz, F.G.M., Heering, H.A. & Dekker, C. Enzyme-Coated Carbon Nanotubes as Single-Molecule Biosensors. *Nano Letters* **3**, 727-730 (2003).

25. Gruner, G. Carbon nanotube transistors for biosensing applications. *Analytical and Bioanalytical Chemistry* **384**, 322-335 (2006).

26. Wang, Y. & Lu, H.P. Bunching effect in single-molecule T4 lysozyme nonequilibrium conformational dynamics under enzymatic reactions. *The Journal of Physical Chemistry B* **114**, 6669-6674 (2010).

27. Svoboda, K., Mitra, P.P. & Block, S.M. Fluctuation analysis of motor protein movement and single enzyme kinetics. *Proceedings of the National Academy of Sciences of the United States of America* **91**, 11782-11786 (1994).

28. Schnitzer, M.J. & Block, S.M. Statistical kinetics of processive enzymes. *Cold Spring Harbor Symposia on Quantitative Biology* **60**, 793-802 (1995).

29. Xu, W., Kong, J.S. & Chen, P. Single-Molecule Kinetic Theory of Heterogeneous and Enzyme Catalysis. *The Journal of Physical Chemistry C* **113**, 2393-2404 (2009).

30. Onuchic, J.N., Luthey-Schulten, Z. & Wolynes, P.G. Theory of protein folding: the energy landscape perspective. *Annual Review of Physical Chemistry* **48**, 545-600 (1997).

31. Chen, Y., Hu, D., Vorpagel, E.R. & Lu, H.P. Probing Single-Molecule T4 Lysozyme Conformational Dynamics by Intramolecular Fluorescence Energy Transfer. *The Journal of Physical Chemistry B* **107**, 7947-7956 (2003).

32. Choi, Y. *et al.* Single Molecule Dynamics of Lysozyme Processing Distinguishes Linear and Cross-linked Peptidoglycan Substrates. *Journal of the Am Chem Soc* in review (2011).

33. Lu, H.P. Revealing time bunching effect in single-molecule enzyme conformational dynamics. *Physical Chemistry Chemical Physics* (2011).doi:10.1039/c0cp02860f

34. Bhabha, G. *et al.* A dynamic knockout reveals that conformational fluctuations influence the chemical step of enzyme catalysis. *Science* **332**, 234-238 (2011).

35. Adamczyk, A.J., Cao, J., Kamerlin, S.C.L. & Warshel, A. Catalysis by dihydrofolate reductase and other enzymes arises from electrostatic preorganization, not conformational motions. *Proceedings of the National Academy of Sciences of the United States of America* **108**, 14115-14120 (2011).

36. Peng, Q. & Li, H. Atomic force microscopy reveals parallel mechanical unfolding pathways of T4 lysozyme: Evidence for a kinetic partitioning mechanism. *Proceedings of the National Academy of Sciences of the United States of America* **105**, 1885-1890 (2008).

37. Llinás, M., Gillespie, B., Dahlquist, F.W. & Marqusee, S. The energetics of T4 lysozyme reveal a hierarchy of conformations. *Nature Structural Biology* **6**, 1072-1078 (1999).

38. Radmacher, M., Fritz, M., Hansma, H.G. & Hansma, P.K. Direct observation of enzyme activity with the atomic force microscope. *Science* **265**, 1577-1579 (1994).

39. Lu, H.P. Single-molecule spectroscopy studies of conformational change dynamics in enzymatic reactions. *Current Pharmaceutical Biotechnology* **5**, 261-269 (2004).

40. Lu, H.P. Single-Molecule Enzymatic Dynamics. *Science* **282**, 1877-1882 (1998).